Analytical Methods

ROYAL SOCIETY OF CHEMISTRY

PAPER

View Article Online
View Journal

Cite this: DOI: 10.1039/d2ay01627c

A portable electrochemical sensing platform for serotonin detection based on surface-modified carbon fiber microelectrodes†

Jinjing Han, [abc] Justin M. Stine,[abc] Ashley A. Chapin [bcd] and Reza Ghodssi*[abcd]

Received 5th October 2022
Accepted 25th January 2023

DOI: 10.1039/d2ay01627c

rsc.li/methods

Serotonin (5-HT) is one of the key neurotransmitters in the human body, regulating numerous physiological functions. A disruption in 5-HT homeostasis could result in serious health problems, including neurodegenerative disorders, depression, and 5-HT syndrome. Detection of 5-HT concentrations in biological fluids, such as urine, is a potential solution for early diagnosis of these diseases. In this study, we developed a novel, simple, and low-cost electrochemical sensing platform consisting of a portable workstation with customized electrodes for 5-HT detection in artificial biological fluids. Nafion/carbon nanotubes (CNTs) and electrochemically modified carbon fiber microelectrodes (Nafion–CNT/EC CFMEs) displayed improved 5-HT sensitivity and selectivity. Together with a customized Ag/AgCl reference electrode and Pt counter electrode, the portable 5-HT sensing platform had a sensitivity of 0.074 μA μM^{-1} and a limit of detection (LOD) of 140 nM. This system was also assessed to measure 5-HT spiked in artificial urine samples, showing nearly full recovery rates. These satisfactory results demonstrated that the portable system exhibits outstanding performance and confirmed the feasibility of 5-HT detection, which can be used to provide point-of-care analysis in actual biological samples.

Introduction

Serotonin (5-HT) is best known as a neurotransmitter in the brain that is involved in a variety of nervous system functions, including mood, fear, feelings of relaxation, mental focus, and learning ability.[1] However, most 5-HT is produced in peripheral tissues (*e.g.*, gastrointestinal tract and pancreas) to regulate metabolic homeostasis, gastrointestinal motility, and bone metabolism.[2–5] Clinical evidence suggests that an abnormal 5-HT level in the human body results in various health problems. For example, 5-HT deficiency is linked with psychiatric disorders, such as major depression and anxiety disorder.[6–9] Likewise, abnormally high 5-HT levels can lead to a potentially life-threatening condition known as 5-HT syndrome. 5-HT syndrome is an adverse reaction induced by an overdose of a serotonergic agent; often, symptoms are recognized and resolved within 24 hours of immediate treatment.[10] Identifying 5-HT concentrations within this timing window through rapid testing is critical for effective treatment. Non-invasive rapid tests usually require samples of body fluids, such as blood, urine, saliva, and nasal secretions. In the body, 5-HT is produced and released into the blood, transported to the kidneys through systemic circulation, and then excreted into the urine.[11,12] Thus, urinary 5-HT is a potential biomarker of 5-HT syndrome,[13] as well as other serotonergic imbalance associated physiological conditions such as depression[11] and carcinoid tumors.[14] Conventional analytical detection methods for urinary 5-HT tests include liquid chromatography/tandem mass spectrometry (LC/MS–MS),[15,16] and enzyme-linked immunosorbent assay (ELISA).[17] Although these methods can detect 5-HT with a low detection limit (~10 nM), they require a series of time-consuming sample preparation procedures, expensive instrumentation, and trained personnel.[18] Advancements in the miniaturization of hardware for electrochemical analysis have facilitated improved sensing capabilities for point-of-care testing in healthcare.[19–26] Given these considerations, a simple, low-cost, and portable urinary 5-HT testing platform would provide a solution for early diagnosis of disease and self-monitoring of health status.

Compared to benchtop instrumentation, these systems possess advantages in portability, simplicity, and cost, enabling rapid detection outside of the laboratory environment.[27–29] Miniaturized potentiostat circuits have been realized and integrated into commercial off-the-shelf (COTS) analog front-end (AFE) chips that can be readily programmed to perform

[a]Department of Electrical and Computer Engineering, University of Maryland, College Park, MD 20742, USA, . E-mail: ghodssi@umd.edu
[b]Institute for Systems Research, University of Maryland, College Park, MD 20742, USA
[c]Robert E. Fischell Institute for Biomedical Devices, University of Maryland, College Park, MD 20742, USA
[d]Fischell Department of Bioengineering, University of Maryland, College Park, MD 20742, USA

† Electronic supplementary information (ESI) available. See DOI: https://doi.org/10.1039/d2ay01627c

electrochemical measurements, enabling a variety of health-related applications.[30–35]

Carbon-based materials have been commonly used for electrochemical measurements due to their excellent properties, such as high electrical and thermal conductivities, and adequate corrosion resistance.[36–38] However, limited sensitivity prevents bare carbon fiber microelectrodes (CFMEs) from directly detecting 5-HT at a physiologically relevant level.[39] Surface modifications are required for CFMEs to achieve fast, precise, selective, and sensitive detection of 5-HT in biological samples. For example, because Nafion is a negatively charged perfluorinated ion-exchange film,[40] Nafion-coated CFMEs show improved selectivity for cationic amines, such as 5-HT, over negatively charged interference molecules like uric acid (UA) or ascorbic acid (AA) during electrostatic interactions.[40–42] Recently, improved electrochemical sensitivity has been demonstrated in CFMEs deposited with carbon nanotubes (CNTs) dispersed in Nafion (Nafion–CNT CFMEs).[43–45] CNTs, cylindrical graphite sheets with nanometer dimensions, provide a large surface-to-volume ratio and surface area. Due to their unique structures, they provide increased sensitivity, electron transfer kinetics, and electrocatalytic activity with minimal surface fouling.[46–48] Thus, Nafion–CNT CFMEs have been used to detect biochemicals such as adenosine (ADN),[43] dopamine (DA),[44,45] and 5-HT[45] in biological samples using benchtop potentiostats with ultra-fast scan rates. However, due to the limited sensitivity of portable potentiostat systems, further electrode surface enhancement is necessary to realize sensitive and selective detection of 5-HT. In addition to surface coatings, surface activations such as thermal activation, mechanical polishing, and electrochemical activation have been applied to carbonaceous electrodes to improve electrochemical performance through the generation of electrochemically active oxygen-rich groups[49] and nanostructures that increase the electroactive surface area.[50,51] Among these activation techniques, electrochemical treatment is preferable for CFMEs as it is a cost-effective and mild process.

In this study, we present the development of a portable sensing platform for 5-HT detection based on a Nafion–CNT and electrochemically treated (Nafion–CNT/EC) CFME with a low-cost potentiostat reader. The Nafion–CNT film was dip-coated on a CFME, and electrochemical treatment was applied to significantly increase the electrode surface area and enhance the 5-HT sensitivity. The Nafion–CNT/EC CFME connects to data analysis software *via* an integrated circuit (IC) for portable 5-HT detection (Fig. 1). Each component of the platform was integrated to achieve selective and sensitive detection of 5-HT using cyclic voltammetry (CV). The developed platform exhibited a sensitivity of 0.074 μA μM^{-1} ($R^2 = 0.9968$) and a limit of detection (LOD) of 140 nM for 5-HT detection, which are comparable to using a commercial benchtop potentiostat. Additionally, the portable system accurately measured 5-HT concentrations in artificial urine samples. Consequently, the Nafion–CNT/EC electrode-based portable 5-HT detection system is promising to satisfy the requirements for point-of-care and self-monitoring applications.

Materials and methods

Chemicals

Serotonin hydrochloride was purchased from Alfa Aesar (Haverhill, MA), and phosphate-buffered saline (PBS) powder was purchased from Research Products International (Mt Prospect, IL). 1X PBS (pH = 7.4) was made by dissolving PBS powder in

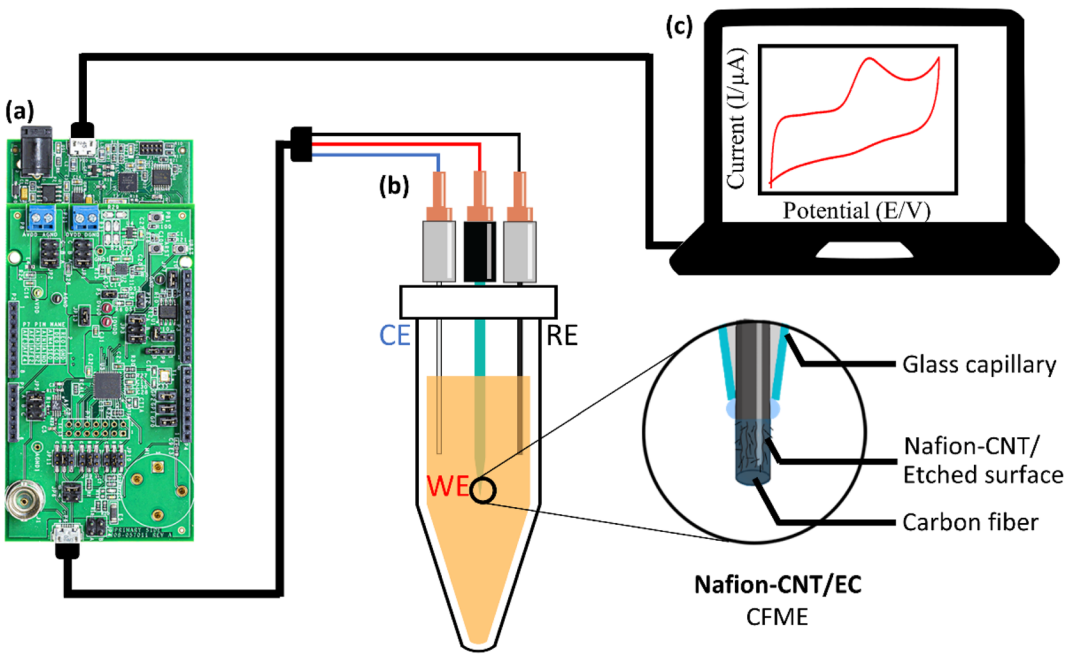

Fig. 1 Schematic illustration of the Nafion–CNT/EC CFME-based portable 5-HT detection system: (a) the IC, (b) the sensing element, and (c) the PC with a software interface.

deionized (DI) water, which was used to prepare 5-HT solutions. Potassium ferricyanide (III) and potassium hexacyanoferrate (II) trihydrate were purchased from Sigma-Aldrich (St. Louis, MO). Single-walled CNTs functionalized with 1.0–3.0 atomic% carboxylic acid (P3-SWNT) were purchased from Carbon Solutions, Inc. (Riverside, CA). A dispersion of 5% Nafion was purchased from Sigma-Aldrich (St. Louis, MO) and diluted in isopropanol. A 0.5 mg mL^{-1} Nafion–CNT solution was made with a suspension of CNTs in 2.5% Nafion solution. Artificial urine (pH = 6.4) recipe[52] can be found in the ESI† (Table S1).

Portable sensing platform

The portable sensing platform integrates an AFE development board, EVAL-AD5941ELCZ (Analog Devices, Wilmington, MA), with a customized three-electrode electrochemical cell. The development board features a potentiostat IC, AD5941, specializing in performing electrochemical measurements as well as an ultra-low power 32-bit ARM Cortex™-M3 processor for event handling and system configuration. A native USB interface is also included, allowing debugging and wired data acquisition *via* a universal synchronous/asynchronous receiver/transmitter (USART). Specifically, the AD5941 (7 mm × 7 mm, 48-lead LFCSP package) consists of internal reference voltage sources, a digital waveform generator, a 16-bit analog to digital converter (ADC), a voltage digital to analog converter (DAC), a transimpedance amplifier (TIA) to measure sensor current output, and a serial peripheral interface (SPI) to facilitate inter board data transfer. A single AD5941 potentiostat IC costs $12, particularly suitable for low-cost portable electrochemical sensing applications.

Generation of CV waveforms

CV waveforms were generated using the portable sensing system from user-provided measurement parameters, such as step size, step duration, number of data points, ramp duration, and TIA resistance. Ideally in CV measurements, the working electrode (WE) potential is ramped linearly *versus* time. However, due to limited DAC capabilities, most measurements are performed in a staircase manner that closely resembles a linear sweep. The AFE initiates the internal DAC to generate and step the excitation voltage, while also recording the readout current between the WE and counter electrode (CE). The step size refers to the incremental change in amplitude of the applied voltage, and the step duration refers to the time delay prior to the next voltage increment, during which the current can be measured. For 5-HT detection, the CV waveform was varied from −0.1 V to +0.6 V with other parameters optimized for improved measurement sensitivity. Considering the hardware limitations such as the minimum step size and duration of the portable sensing platform, a scan rate of 200 mV s^{-1} was used, resulting in a step size of 1.75 mV, step duration of 8.75 ms, 800 total recorded data points, and a ramp duration of 7 s. The peak current was estimated to be ∼1 μA during 5-HT sensing, so the TIA resistance was set to 512 kΩ to maximize measurement accuracy. The generated waveform was confirmed using an oscilloscope (Tektronix, OR).

CFME fabrication and modifications

The surface of the T-650 carbon fiber (Solvay, TX) was modified with Nafion–CNT and an electrochemical treatment to improve its sensitivity and selectivity. A single fiber was inserted into a glass capillary with an inner diameter of 0.4 mm (A-M Systems, WA). The carbon fiber was sealed using epoxy and cut down to a 5 mm tip. Copper wire (30 AWG) was inserted into the glass capillary from the backside. A 0.5 mg mL^{-1} Nafion–CNT solution was sonicated for 30 min before each use to re-suspend the nanotubes. CFMEs were coated with the Nafion–CNT film by dip-coating and were air-dried for 30 minutes before use. The electrochemical treatment consisted of applying two repeated CV waveforms of 0 to +2.5 V and 0 to −1.5 V at a scan rate of 100 mV s^{-1}. The Nafion–CNT CFMEs were only modified with dip-coated Nafion–CNT and the Nafion–CNT/EC CFMEs were modified with dip-coating Nafion–CNT, followed by electrochemical treatment.

Ag/AgCl reference electrode (RE) and Pt CE construction

The Ag/AgCl RE was fabricated by coating AgCl on a bare Ag wire (32 AWG, A-M Systems, WA). An Ag wire and Pt wire (36 AWG, A-M Systems, WA) were partially immersed (∼1 cm) in 1 M KCl solution and connected to the WE and RE/CE of the benchtop VSP-300 potentiostat (BioLogic, France), respectively. A 0.15 mA current was applied to the WE to chloride the surface until a uniform AgCl coating was formed. Both Ag/AgCl RE and Pt CE were inserted into glass capillaries with a 1 cm tip extended.

Surface characterization

All scanning electron microscopy (SEM) images and energy-dispersive X-ray spectra (EDS) were acquired in the University of Maryland Nanocenter AIMlab using a Tescan GAIA instrument. The CFME samples were prepared and attached to a clean Si wafer using carbon tape for surface characterization. The SEM images were recorded with an accelerating voltage of 10.0 kV and a working distance of approximately 5 mm.

Electrochemical measurements

The surface-modified CFMEs were first characterized by CV with a benchtop potentiostat (VSP-300, BioLogic, France) to determine the electrode surface area and signal response to 5-HT in an electrochemical cell with a standard Ag/AgCl/3 M KCl RE and a Pt CE (CH Instruments, Austin, TX). Measurements from the developed portable electrochemical sensing platform were compared to measurements from a standard benchtop apparatus and used to determine 5-HT in artificial urine samples. The interference study was carried out with the benchtop potentiostat with customized electrodes. All collected data are analyzed using MATLAB.

Results and discussion

Surface characterization of modified CFMEs

The surface morphologies of bare, Nafion–CNT, and Nafion–CNT/EC CFMEs were characterized using an SEM. The bare

CFME (Fig. 2a) showed a smooth surface with striation, which is typical of the polyacrylonitrile (PAN) manufacturing process used to fabricate carbon fibers. The Nafion–CNT modified CFME (Fig. 2b) added a thin, dense coating of CNT on the electrode surface. With further electrochemical treatment, the Nafion–CNT/EC CFME (Fig. 2c) produced even rougher surface striations as a result of the electrochemical etching effect, while still retaining the Nafion–CNT film. The SEM images suggested that the Nafion–CNT dip coating and further electrochemical treatment produced nanostructures with an increased surface area.

EDS analysis was used to obtain detailed information on the elemental composition of modified electrodes (Fig. 2d–f). Carbon content was confirmed on the bare CFME with trace amounts of oxygen (Fig. 2d). The presence of oxygen on the CFME was not unexpected and may originate from the thin epoxy protective layer that resides on the surface during the fiber sizing process. Increased oxygen content was observed on the surface of the sample following each successive surface modification step. Specifically, during dip-coating of the CFME in Nafion–CNT (Fig. 2e) oxygen likely originated from the carboxylic acid functional groups on the CNTs and from the $-SO_3$ groups of the Nafion film. Additionally, electrochemical treatment further increased the oxygen content (Fig. 2f), which may indicate the addition of oxygen functional groups to the CFME surface during the electrochemical etching process.[49,53] The Nafion–CNT/EC CFMEs also showed a clear peak of fluorine, indicating remnants of the Nafion coating after the electrochemical treatment. Silicon was present across all samples due to the use of a silicon substrate holder for EDS analysis and was not from the sample itself.

To estimate the electroactive surface area (EASA) of surface-modified CFMEs, equimolar 10 mM potassium ferrocyanide ($K_4[Fe(CN)_6]$) and potassium ferricyanide ($K_3[Fe(CN)_6]$) were used because their electrochemical sensitivity is highly relevant to the defects/edge plane sites.[54] CV was performed at various scan rates from 50 mV s^{-1} to 250 mV s^{-1}, and the resulting currents were plotted against the square root of scan rates (Fig. 3). Visible changes in the shape of the cyclic voltammograms were apparent after each step of surface modification. In Fig. 3a, before surface modification, the bare CFME shows a poorly defined CV current plateau with a high linear background and almost no peak current. After Nafion–CNT coating, a poorly defined plateau with linear background remains, but the peak is more distinguishable than that of the bare electrode. After further electrochemical treatment, the Nafion–CNT/EC CFME illustrates a well-defined steady-state plateau with measurable peaks. The changes in the shape of cyclic

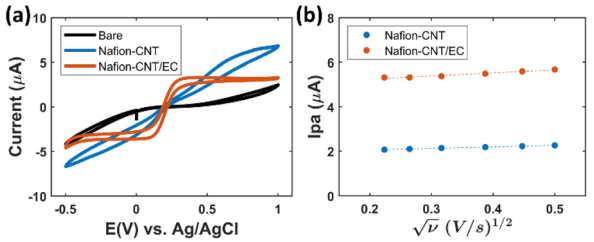

Fig. 3 Comparison of CV properties of bare and modified CFMEs. (a) Cyclic voltammograms of 10 mM ferricyanide/ferrocyanide at bare, Nafion–CNT, and Nafion–CNT/EC CFMEs, at a scan rate of 250 mV s^{-1}. (b) Linear regression of I_{pa} *vs.* the square root of scan rates of 50, 70, 100, 150, 200, and 250 mV s^{-1}. $R^2 = 0.9982$ and 0.9719 for Nafion–CNT and Nafion–CNT/EC, respectively.

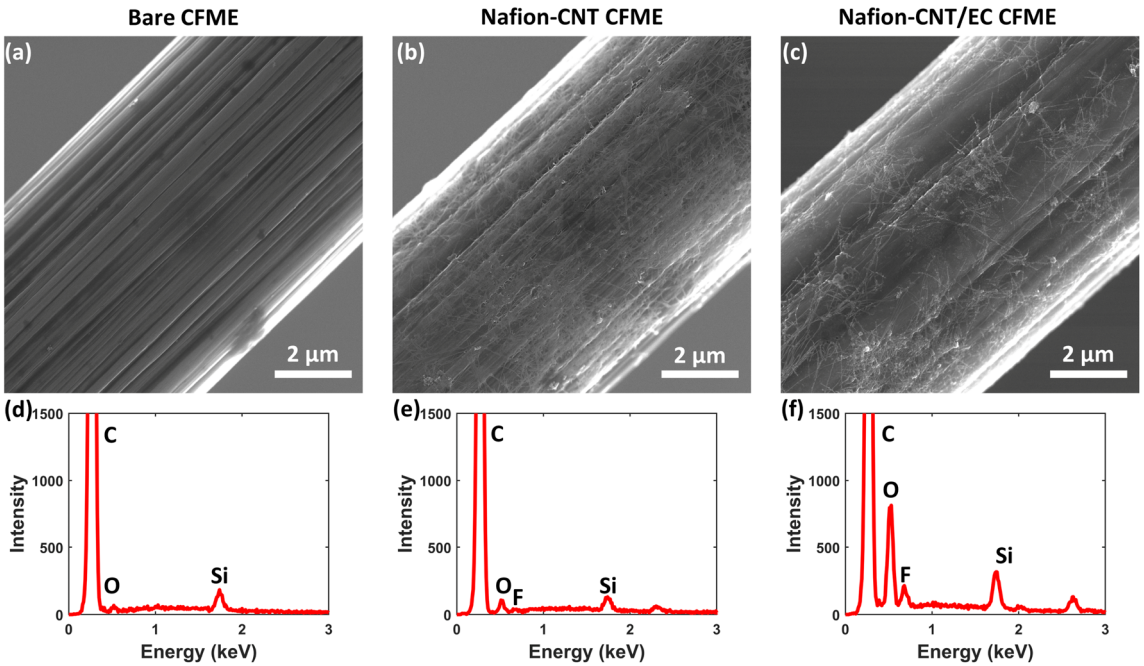

Fig. 2 (a–c) SEM images and (d–f) EDS analysis of bare, Nafion–CNT and Nafion–CNT/EC CFMEs.

voltammograms of ferricyanide/ferrocyanide at the CFMEs after surface modifications are direct indications of changes in the surface electrochemical properties resulting from Nafion–CNT coating and electrochemical treatment.

The plot of oxidation peak current (I_{pa}) *versus* the square root of the scan rate ($\nu^{1/2}$) is shown in Fig. 3b. The linear relationship between I_{pa} and $\nu^{1/2}$ suggests a diffusion-controlled detection of ferricyanide/ferrocyanide on the CFME surface. For a diffusion-controlled electrochemical reaction, the EASA can be estimated using the Randles–Sevcik equation (eqn (1)). It is worthwhile to mention that the shape of the CV does not resemble the waveform expected for a microelectrode, where the reverse sweep of the voltammogram closely overlaps the forward one. In contrast, the measurement curve depicts a transition between microelectrode and macroelectrode behavior, possibly due to high surface roughness, large surface area, and fast scan rates. Compton *et al.* have shown that at fast scans rates, regardless of the geometry of the electrodes, the voltammetry would show a peaked response with a peak current given by the Randles–Sevcik equation.[55]

$$I_{pa} = 0.4463nFAC\left(\frac{nFvD}{RT}\right)^{1/2} \quad (1)$$

Based on the slope calculated from Fig. 3, the EASAs for Nafion–CNT and Nafion–CNT/EC CFME are estimated to be 3.9 $\times$ 10^{-5} cm^2 and 9.2 $\times$ 10^{-5} cm^2 respectively. Due to the thin Nafion–CNT coating layer and rough surface, the calculated EASAs may be underestimated since the Randles–Sevcik equation is best used to model planar surfaces. However, the estimated value indicates that electrochemical treatment increases the EASA. Conversely, the bare electrode is not electrochemically responsive to ferricyanide/ferrocyanide. This may be attributed to the thin epoxy layer (1% UC.309 epoxy) coated during carbon fiber fabrication, blocking electron transfer. The shape of the CVs also indicates slower rate constants and electron transfer at the bare and Nafion–CNT CFMEs, compared to Nafion–CNT/EC. The increased EASA may be attributed to the electrochemical etching effect which removed the epoxy layer and generated nanostructured surface texture on the carbon fiber and CNT film.[50,51] Both Nafion–CNT coating and electrochemical treatment enhance electrochemical properties, including improving the shape of the CV curve and increasing I_{pa} values, which increase the sensitivity to electrochemically active species. Overall, the Nafion-CNT/EC CFMEs provide the highest EASA.

Surface-modified CFMEs increase signal response to 5-HT

To evaluate the electrochemical performance of surface-modified CFMEs in 5-HT detection, CFMEs with different surface modifications were compared using CVs (Fig. 4). The Nafion–CNT CFMEs showed an increased I_{pa} in 10 μM 5-HT (0.139 ± 0.03 μA) at oxidation peak potential E_{pa} = 0.43 V, compared to the bare CFMEs (0 ± 0.001 μA). Further electrochemical treatment dramatically increased both background current and I_{pa} to 5-HT (0.676 ± 0.029 μA) at the same E_{pa}, showing a 4.9-fold increase in I_{pa}. The increased background

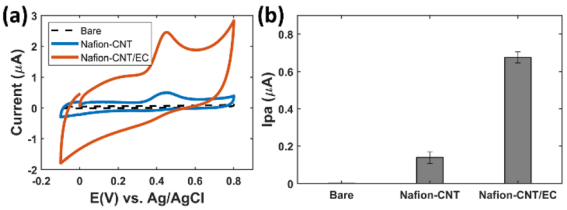

Fig. 4 CV response of modified CFMEs in PBS and 5-HT. (a) Faradaic current response to 10 μM 5-HT in PBS. (b) Average I_{pa}s in the detection of 10 μM 5-HT using bare, Nafion–CNT, and Nafion–CNT/EC modified CFMEs. Error bars denote standard error (n = 6). Potential range: −0.1 to 0.8 V. Scan rate: 1 V s^{-1}.

signal after electrochemical treatment suggests increased double-layer capacitance, indicating higher EASA. Overall, CFMEs with Nafion–CNT coating and electrochemical treatment indicated an excellent signal response to 5-HT compared to bare and Nafion–CNT CFMEs. The error bars in I_{pa} were expected to be caused by variations in the dip-coating and electrochemical treatment processes.

To determine the improvement in 5-HT sensitivity due to electrochemical treatment, 5-HT sensitivity was compared between Nafion–CNT and Nafion–CNT/EC CFMEs (Fig. S1†) using a benchtop potentiostat. The Nafion–CNT electrodes showed a linear range between 200 and 800 nM, while the Nafion–CNT/EC electrodes displayed a linear range between 100 and 800 nM. The slope of this linear region denotes 5-HT sensitivity, and the sensitivity of the Nafion–CNT/EC CFME is calculated as 84.6 nA μM^{-1} (R^2 = 0.9911). The LOD is obtained as 3 × resolution/sensitivity = (3 × 0.52 nA)/(84.6 nA μM^{-1}) = 17 nM, and the limit of quantification (LOQ) is calculated to be 56 nM. The Nafion–CNT CFME has a sensitivity of 7.23 nA μM^{-1} (R^2 = 0.8880). The LOD is obtained with the same calculation = (3 × 1.51 nA)/(7.23 nA μM^{-1}) = 626.5 nM, with a LOQ of 2.07 μM. Overall, the Nafion–CNT/EC CFMEs showed significantly improved sensitivity (11.7×) and LOD (36.9×) for 5-HT detection compared to the Nafion–CNT CFMEs.

The improved 5-HT detection by surface modifications may be explained by the following mechanisms: (1) increased surface charges, (2) increased surface area and defects/edge plane sites, and (3) increased oxygen functional groups generated on the surface. Coating CFMEs with Nafion and carboxylic acid-functionalized CNTs provides additional negative charges, availability of edge plane active sites for adsorption, and conductivity and electron transfer due to the addition of oxygen atoms with an open π orbital.[56,57] Similarly, the electrochemical treatment also creates negative charges, defects/edge plane sites, and adds oxygen-containing functional groups to the surface.[53] The use of both treatments enhances 5-HT detection significantly. Therefore, the Nafion–CNT/EC CFMEs are optimal for electrochemical measurements using portable potentiostat electronics.

Interference, fouling, and pH study for surface-modified CFMEs

Accurate detection of 5-HT in biological samples is hindered by interfering electroactive molecules such as 5-

hydroxyindoleacetic acid (5-HIAA), UA, DA, norepinephrine (NE), and ADN.[58] In this work, these interfering molecules were mixed with 5-HT and the I_{pa}s of CV responses were recorded on Nafion–CNT/EC CFMEs to explore the selectivity of this analytical approach. Fig. 5 illustrates that a 10-fold concentration of 5-HIAA, UA, NE, ADN and a 20-fold concentration of DA had little influence over the detection of 5-HT, where the differences in I_{pa}s were within 7%.

5-HT is known to foul the electrode and reduce the sensitivity. Thus, Nafion–CNT/EC CFMEs were used to measure 1 μM 5-HT for 30 consecutive cycles for reproducibility tests. The results indicated that the current response I_{pa}s varied between 101.9% and 89.6% of the initial value (Fig. S3†). The electrodes can be readily replaced to restore measurement precision, minimizing the impact of fouling.

The impact of pH on 5-HT detection was also investigated. The same electrode was tested for sensitivity in 5-HT solution with pHs of 6.0 and 7.4. The results (Fig. S4†) showed a 27% increase in sensitivity for the lower pH condition. Variations in sensor performance are potentially due to different reaction rates with respect to pH. Thus, in practice, the effects of pH should be considered and a re-calibration in targeted pH is recommended.

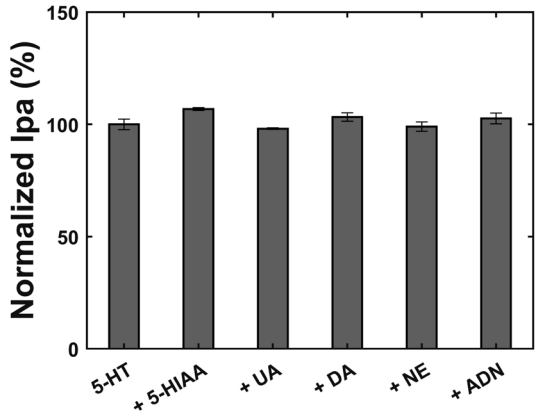

Fig. 5 Selectivity of Nafion–CNT/EC CFMEs. Average normalized I_{pa}s of 5-HT coexisting with different interfering substances: 1 μM 5-HT (100%); 1 μM 5-HT + 10 μM 5-HIAA (107%); 1 μM 5-HT + 10 μM UA (98%); 1 μM 5-HT + 20 μM DA (103%); 1 μM 5-HT + 10 μM NE (99%); 1 μM 5-HT + 10 μM ADN (103%). I_{pa}s are normalized to 1 μM 5-HT. Potential range: −0.1 to 0.6 V. Scan rate: 200 mV s^{-1}.

Comparison of portable and benchtop apparatus

The portable electrochemical sensing platform for 5-HT detection comprises a three-electrode system, an IC potentiostat, and a PC with software for data analysis (Fig. 6). To evaluate its electrochemical performance, the potentiostat circuit and customized electrodes were compared to their standard counterparts, separately and integrated, to determine 5-HT sensitivity.

The portable AD5941 IC was compared to a high-end VSP-300 benchtop potentiostat in 10 mM $K_3[Fe(CN)_6]/K_4[Fe(CN)_6]$ as a benchmark. Fig. 7a compares the cyclic voltammograms that were recorded using a VSP-300 and AD5941 IC. The 5-HT E_{pa}s were observed to be 0.49 V for both instruments, while I_{pa}s were 175 μA and 190 μA from the benchtop and portable potentiostats, respectively. Similar E_{pa}s and I_{pa}s demonstrated the viability of using the portable IC for reliable CV measurements. Customized RE and CE were compared with their standard commercial Ag/AgCl/3 M KCl RE and Pt wire CE counterparts in 10 μM 5-HT (Fig. S2†). The customized electrodes showed identical I_{pa}s and a 29 mV potential shift to the left compared to the standard electrodes. This result implied that the customized

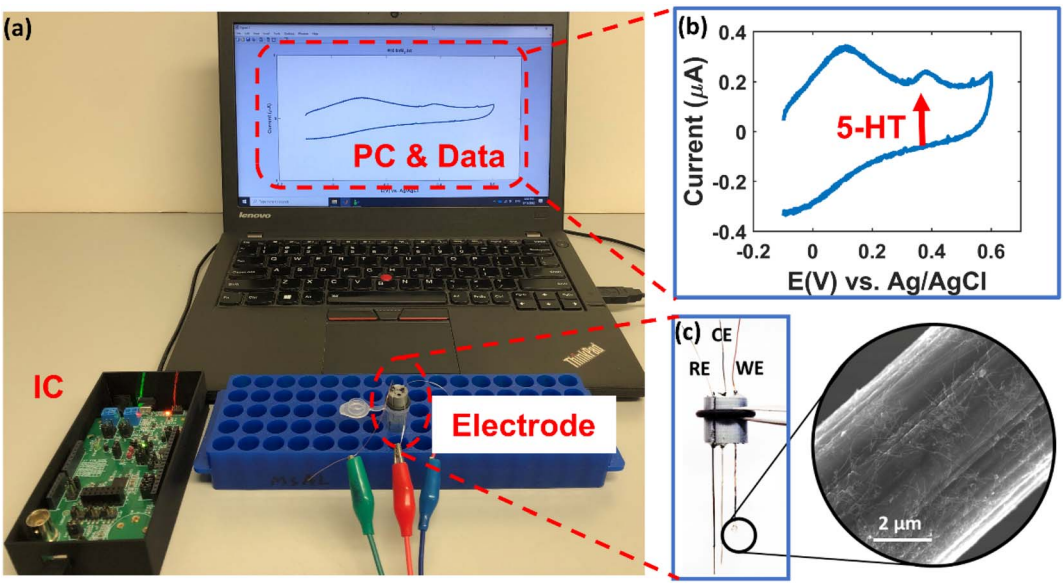

Fig. 6 (a) Photograph of the portable electrochemical 5-HT sensing platform, comprising PC, IC, and customized electrodes. (b) Software interface showing representative CV. (c) Customized three-electrode system, including Nafion–CNT/EC WE with SEM, Ag/AgCl RE, and Pt CE.

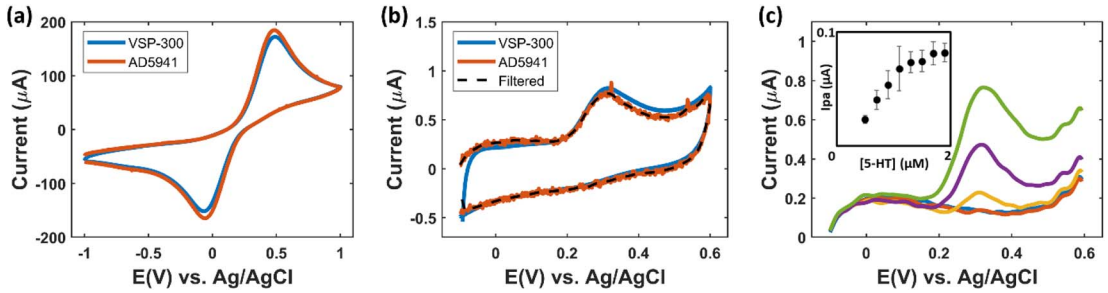

Fig. 7 (a) Comparison of the AD5941 IC to a VSP-300 benchtop potentiostat for CV sensing of 10 mM $K_3[Fe(CN)_6]/K_4[Fe(CN)_6]$. Potential range: −1 to 1 V. Scan rate: 100 mV s^{-1}. Standard glassy carbon as WE, Ag/AgCl/3 M KCl as RE, Pt as CE. (b) Cyclic voltammograms comparing the AD5941 and benchtop potentiostat in 10 μM 5-HT. Potential range: −0.1 to 0.6 V. Scan rate: 200 mV s^{-1}. Nafion–CNT/EC as WE, customized Ag/AgCl as RE, Pt as CE. (c) Cyclic voltammograms of 5-HT concentrations (0.1–10 μM) using the portable system consisting of Nafion–CNT/EC and AD5941. Potential range: −0.1 to 0.6 V. Scan rate: 200 mV s^{-1}. Nafion–CNT/EC as WE, customized Ag/AgCl as RE, Pt as CE. [5-HT]: 0.1 μM (blue), 0.5 μM (orange), 1 μM (yellow), 5 μM (purple), and 10 μM (green). Inset: calibration curve of 5-HT with a linear range of 0.5 to 1.1 μM.

electrodes perform similarly to the standard RE/CE, except for a slight peak shift likely due to the difference in RE potentials.

The surface-modified CFMEs with a customized RE and CE were configured with portable electronics and used for 5-HT detection and their electrochemical performances were compared with a benchtop potentiostat (Fig. 7b). Cyclic voltammograms of 10 μM 5-HT recorded by the benchtop and portable potentiostats had similar peak shapes, E_{pa}s (0.31 V for both), and I_{pa}s (0.41 μA for the benchtop potentiostat, and 0.37 μA for the portable potentiostat) using customized electrodes.

The sensitivity of the portable sensing platform system was also characterized. A calibration curve over 5-HT concentrations 0.1–10 μM (Fig. 7c) showed a linear range of 0.5–1.1 μM with a sensitivity of 0.074 μA μM^{-1} ($R^2 = 0.9968$), LOD of 140 nM, and LOQ of 420 nM. These results demonstrate the ability of the reported portable sensing system to reliably detect sub-micromolar 5-HT levels. The analytical characterization of this portable 5-HT sensing system in comparison with literature data is summarized in Table S2.†[59–66] Although other reports show superior performance with lower LODs, they require expensive (~$10 000) and customized potentiostat hardware to generate faster scan rates and process large data sets to improve the LOD.[59–61] This low-cost (~$300), portable system shows an improved LOD compared to other portable systems for neurotransmitter detection, such as 5-HT and DA. Additionally, the performance of the proposed system is sufficient to detect 5-HT in urine samples (normal range between 0.27 and 1.65 μM),[67] thereby providing an alternative point-of-care solution.

Detection of 5-HT in artificial urine samples using the portable sensing system

5-HT is involved in a wide variety of physiological functions. The reference level for the urinary 5-HT test is 600 nM,[68] and increased 5-HT levels in urine may confirm the diagnosis of 5-HT syndrome[13] or indicate the presence of a carcinoid tumor in the gastrointestinal tract.[14] This study investigated the applicability of the developed portable system for 5-HT detection in artificial urine, showcasing its application for point-of-care diagnostics.

The determination of 5-HT in artificial urine samples was investigated using CV on a Nafion–CNT/EC-based portable electrochemical sensing platform using the standard addition method. The CV responses to the direct addition of 5-HT (0.1–1 μM) in artificial urine were used to determine the recovery of 5-HT from artificial urine (Fig. 8). While cyclic voltammograms recorded in artificial urine alone revealed no peak, when 5-HT was added, a well-defined anodic peak at +0.38 V was observed. The intensities of the peaks were correlated with 5-HT concentrations and increased with the successive addition of standard 5-HT solution into the artificial urine sample. 5-HT concentrations and their recovery rates were calculated based on the previously determined calibration curve. The spiked 5-HT concentrations were found to be between 0.3 μM and 1.0 μM, with recovery rates ranging from 74% to 105% (Table 1). The average recovery rate at low concentration exceeds 100%, which may be caused by variations between electrodes and interference molecules in the artificial urine samples, while the decrease in average recovery rate at higher concentrations may be caused by 5-HT fouling.[48] Overall, these recovery analysis results are similar to the recommended range (80–120%),[69]

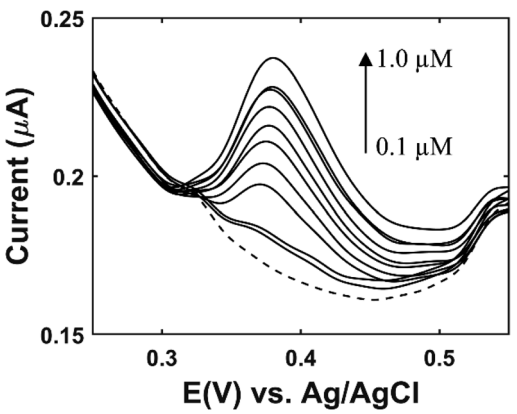

Fig. 8 Cyclic voltammograms of 5-HT recorded at the Nafion–CNT/EC-based portable sensing platform in artificial urine (dashed line) spiked with 5-HT (solid line) at various concentrations (0.1 μM–1.0 μM). Potential range: −0.1 to 0.6 V. Scan rate: 200 mV s^{-1}.

Table 1 Recovery rates and relative standard deviation (RSD) data obtained for 5-HT in artificial urine samples

[5-HT] added (μM)	[5-HT] found (μM)	Average recovery	RSD
0.30	0.30	100%	2.63%
0.40	0.42	105%	0.90%
0.50	0.48	96%	1.10%
0.60	0.57	95%	0.63%
0.70	0.62	89%	0.47%
0.80	0.67	84%	0.47%
0.90	0.68	76%	0.13%
1.00	0.74	74%	0.84%

showing that the proposed method can be used efficiently for the determination of trace amounts of 5-HT directly from urine samples at low concentrations.

Conclusions

In this study, a portable electrochemical sensing platform for 5-HT detection in the artificial biological fluid was developed and characterized. The portable platform showed a LOD of 140 nM with a sensitivity of 0.074 μA μM^{-1} ($R^2 = 0.9968$) in the linear range of 0.5 μM to 1.1 μM, which is physiologically relevant. The selectivity of the sensor was confirmed in the presence of an excess of interfering molecules including 5-HIAA, UA, DA, NE, and ADN. The applicability of the platform in artificial urine was investigated, revealing excellent recovery rates. The experimental results indicate that the portable 5-HT detection system, based on a Nafion–CNT/EC electrode, provides sensitive electrochemical 5-HT measurements as a low-cost, simple, rapid, and versatile point-of-care solution to detect 5-HT. In the future, the electrochemical portable sensing system would be further miniaturized to achieve a smaller footprint and optimized to promote continuous monitoring of 5-HT levels in humans or animals as a wearable or implantable device.

Author contributions

Jinjing Han: conceptualization, data curation, formal analysis, investigation, methodology, software, validation, writing – original draft. Justin M. Stine: investigation, methodology, software, validation, writing – reviewing and editing. Ashley A. Chapin: conceptualization resources, writing – reviewing and editing. Reza Ghodssi: conceptualization, funding acquisition, project administration, supervision, writing – reviewing and editing.

Conflicts of interest

The authors declare that they have no conflict of interest.

Acknowledgements

The authors acknowledge financial support from National Science Foundation grant NCS #1926793. We thank the Maryland Nanocenter and the Advanced Imaging and Microscopy Laboratory (AIMlab) for their assistance taking the SEM images. Special thanks to Dr Jens Herberholz and Norma Peña-Flores for helpful discussions.

References

1 T. A. Jenkins, J. C. D. Nguyen, K. E. Polglaze and P. P. Bertrand, *Nutrients*, 2016, **8**, 56.
2 R. El-Merahbi, M. Löffler, A. Mayer and G. Sumara, *FEBS Lett.*, 2015, **589**, 1728–1734.
3 D. M. Kendig and J. R. Grider, *Neurogastroenterol. Motil.*, 2015, **27**, 899.
4 S. N. Spohn and G. M. Mawe, *Nat. Rev. Gastroenterol. Hepatol.*, 2017, **14**, 412.
5 N. Terry and K. G. Margolis, *Handb. Exp. Pharmacol.*, 2017, **239**, 319.
6 A. Baranyi, O. Amouzadeh-Ghadikolai, D. von Lewinski, R. J. Breitenecker, H.-B. Rothenhäusler, C. Robier, M. Baranyi, S. Theokas and A. Meinitzer, *PeerJ*, 2017, **5**, e3968.
7 M. S. Whitney, A. M. Shemery, A. M. Yaw, L. J. Donovan, J. D. Glass and E. S. Deneris, *J. Neurosci.*, 2016, **36**, 9828–9842.
8 B. D. Sachs, R. M. Rodriguiz, W. B. Siesser, A. Kenan, E. L. Royer, J. P. R. Jacobsen, W. C. Wetsel and M. G. Caron, *Int. J. Neuropsychopharmacol.*, 2013, **16**, 2081.
9 R. Shah, E. Courtiol, F. X. Castellanos and C. M. Teixeira, *Front. Behav. Neurosci.*, 2018, **12**, 114.
10 J. Volpi-Abadie, A. M. Kaye and A. D. Kaye, *Ochsner J.*, 2013, **13**, 533.
11 M. I. Nichkova, H. Huisman, P. M. Wynveen, D. T. Marc, K. L. Olson and G. H. Kellermann, *Anal. Bioanal. Chem.*, 2012, **402**, 1593–1600.
12 D. T. Marc, J. W. Ailts, D. C. A. Campeau, M. J. Bull and K. L. Olson, *Neurosci. Biobehav. Rev.*, 2011, **35**, 635–644.
13 M. Brvar, D. Stajer, G. Kozelj, J. Osredkar, M. Mozina and M. Bunc, *Clin. Toxicol.*, 2007, **45**, 458–460.
14 J. M. Feldman, *Clin. Chem.*, 1986, **32**, 840–844.
15 W. H. A. A. De Jong, M. H. L. I. L. I. Wilkens, E. G. E. E. De Vries and I. P. Kema, *Anal. Bioanal. Chem.*, 2010, **396**, 2609.
16 M. Moriarty, A. Lee, B. O'Connell, A. Kelleher, H. Keeley and A. Furey, *Anal. Bioanal. Chem.*, 2011, **401**, 2481–2493.
17 M. I. Nichkova, H. Huisman, P. M. Wynveen, D. T. Marc, K. L. Olson and G. H. Kellermann, *Anal. Bioanal. Chem.*, 2012, **402**, 1593–1600.
18 E. Johnsen, S. Leknes, S. R. Wilson and E. Lundanes, *Sci. Rep.*, 2015, **5**, 9308.
19 E. T. S. G. da Silva, D. E. P. Souto, J. T. C. Barragan, J. F. Giarola, A. C. M. de Moraes and L. T. Kubota, *ChemElectroChem*, 2017, **4**, 778–794.
20 J. R. Choi, *Front. Chem.*, 2020, **8**, 517.
21 W. Li, W. Luo, M. Li, L. Chen, L. Chen, H. Guan and M. Yu, *Front. Chem.*, 2021, **9**, 723186.
22 J. Xie, D. Cheng, P. Li, Z. Xu, X. Zhu, Y. Zhang, H. Li, X. Liu, M. Liu and S. Yao, *ACS Appl. Nano Mater.*, 2021, **4**, 4853–4862.

23 D. Cheng, P. Li, X. Zhu, M. Liu, Y. Zhang and Y. Liu, *Chin. J. Chem.*, 2021, **39**, 2181–2187.
24 S. Zhang, N. Huang, Q. Lu, M. Liu, H. Li, Y. Zhang and S. Yao, *Biosens. Bioelectron.*, 2016, **77**, 1078–1085.
25 N. Huang, S. Zhang, L. Yang, M. Liu, H. Li, Y. Zhang and S. Yao, *ACS Appl. Mater. Interfaces*, 2015, **7**, 17935–17946.
26 M. Liu, Q. Chen, C. Lai, Y. Zhang, J. Deng, H. Li and S. Yao, *Biosens. Bioelectron.*, 2013, **48**, 75–81.
27 K. Jackowska and P. Krysinski, *Anal. Bioanal. Chem.*, 2013, **405**, 3753.
28 A. Heller and B. Feldman, *Chem. Rev.*, 2008, **108**, 2482–2505.
29 D. Grieshaber, R. MacKenzie, J. Vörös and E. Reimhult, *Sensors*, 2008, **8**, 1400.
30 E. Saygili, B. Orakci, M. Koprulu, A. Demirhan, E. Ilhan-Ayisigi, Y. Kilic and O. Yesil-Celiktas, *Anal. Biochem.*, 2020, **591**, 113538.
31 J. Piedras, R. B. Dominguez and J. M. Gutiérrez, *Chemosensors*, 2021, **9**, 73.
32 A. F. D. Cruz, N. Norena, A. Kaushik and S. Bhansali, *Biosens. Bioelectron.*, 2014, **62**, 249–254.
33 A. Gevaerd, E. Y. Watanabe, C. Belli, L. H. Marcolino-Junior and M. F. Bergamini, *Sens. Actuators, B*, 2021, **332**, 129532.
34 O. S. Hoilett, J. F. Walker, B. M. Balash, N. J. Jaras, S. Boppana and J. C. Linnes, *Sensors*, 2020, **20**, 2407.
35 A. Butterworth, D. K. Corrigan and A. C. Ward, *Anal. Methods*, 2019, **11**, 1958–1965.
36 L. Lu, L. Liang, K. Teh, Y. Xie, Z. Wan and Y. Tang, *Sensors*, 2017, **17**, 725.
37 R. Forster, in *Encyclopedia of Applied Electrochemistry*, ed. G. Kreysa, K. Ota and R. F. Savinell, Springer New York, New York, NY, 2014, pp. 1248–1256.
38 A. R. Pereira, J. C. P. de Souza, R. M. Iost, F. C. P. F. Sales and F. N. Crespilho, *J. Electroanal. Chem.*, 2016, **780**, 396–406.
39 S. Sharma, N. Singh, V. Tomar and R. Chandra, *Biosens. Bioelectron.*, 2018, **107**, 76–93.
40 Z. Tavakolian-Ardakani, O. Hosu, C. Cristea, M. Mazloum-Ardakani and G. Marrazza, *Sensors*, 2019, **19**, 2037.
41 P. Hashemi, E. C. Dankoski, J. Petrovic, R. B. Keithley and R. M. Wightman, *Anal. Chem.*, 2009, **81**, 9462–9471.
42 J. E. Baur, E. W. Kristensen, L. J. May, D. J. Wiedemann and R. M. Wightman, *Anal. Chem.*, 1988, **60**, 1268–1272.
43 A. E. Ross and B. J. Venton, *Analyst*, 2012, **137**, 3045.
44 S. B. Hocevar, J. Wang, R. P. Deo, M. Musameh and B. Ogorevc, *Electroanalysis*, 2005, **17**, 417–422.
45 B. E. K. Swamy and B. J. Venton, *Analyst*, 2007, **132**, 876.
46 S. K. Vashist, D. Zheng, K. Al-Rubeaan, J. H. T. Luong and F.-S. Sheu, *Biotechnol. Adv.*, 2011, **29**, 169–188.
47 J. Wang, *Electroanalysis*, 2005, **17**, 7–14.
48 A. A. Chapin, P. R. Rajasekaran, D. N. Quan, L. Hu, J. Herberholz, W. E. Bentley and R. Ghodssi, *Microsyst. Nanoeng.*, 2020, **6**, 1–13.
49 R. C. Engstrom, *Anal. Chem.*, 1982, **54**, 2310–2314.
50 G. E. Cabaniss, A. A. Diamantis, W. R. Murphy, R. W. Linton and T. J. Meyer, *J. Am. Chem. Soc.*, 1985, **107**, 1845–1853.
51 J. Wang, X. Cai, C. Jonsson and M. Balakrishnan, *Electroanalysis*, 1996, **8**, 20–24.
52 R. C. Huiszoon, J. Han, S. Chu, J. M. Stine, L. A. Beardslee and R. Ghodssi, *IEEE Trans. Biomed. Eng.*, 2021, **68**, 3241–3249.
53 Y. Li, J. Zhou, J. Song, X. Liang, Z. Zhang, D. Men, D. Wang and X.-E. Zhang, *Biosens. Bioelectron.*, 2019, **144**, 111534.
54 R. L. McCreery, *Chem. Rev.*, 2008, **108**, 2646–2687.
55 R. G. Compton, E. Laborda and K. R. Ward, *Understanding Voltammetry*, IMPERIAL COLLEGE PRESS, 2014.
56 Q. Cao, D. K. Hensley, N. V. Lavrik and B. J. Venton, *Carbon*, 2019, **155**, 250–257.
57 C. B. Jacobs, T. L. Vickrey and B. J. Venton, *Analyst*, 2011, **136**, 3557.
58 T. Fukuda, H. Muguruma, H. Iwasa, T. Tanaka, A. Hiratsuka, T. Shimizu, K. Tsuji and T. Kishimoto, *Anal. Biochem.*, 2020, **590**, 113533.
59 K. E. Dunham and B. J. Venton, *Analyst*, 2020, **145**, 7437–7446.
60 A. Abdalla, C. W. Atcherley, P. Pathirathna, S. Samaranayake, B. Qiang, E. Peña, S. L. Morgan, M. L. Heien and P. Hashemi, *Anal. Chem.*, 2017, **89**, 9703–9711.
61 M. Satyanarayana, K. Koteshwara Reddy and K. Vengatajalabathy Gobi, *Electroanalysis*, 2014, **26**, 2365–2372.
62 X. Shen, F. Ju, G. Li and L. Ma, *Sensors*, 2020, **20**, 2781.
63 L. O. Orzari, R. Cristina de Freitas, I. Aparecida de Araujo Andreotti, A. Gatti and B. C. Janegitz, *Biosens. Bioelectron.*, 2019, **138**, 111310.
64 Y. Li, Z. Li, H. Liu, S. Chen, X. Guo, M. Lin and F. Li, *J. Electrochem. Soc.*, 2019, **166**, B524–B531.
65 J. E. Koehne, M. Marsh, A. Boakye, B. Douglas, I. Y. Kim, S. Y. Chang, D. P. Jang, K. E. Bennet, C. Kimble, R. Andrews, M. Meyyappan and K. H. Lee, *Analyst*, 2011, **136**, 1802–1805.
66 S. D. Adams, E. H. Doeven, S. J. Tye, K. E. Bennet, M. Berk and A. Z. Kouzani, *IEEE Trans. Neural Syst. Rehabil. Eng.*, 2020, **28**, 133–142.
67 S. Boonkaew, A. Dettlaff, M. Sobaszek, R. Bogdanowicz and M. Jönsson-Niedziółka, *J. Electroanal. Chem.*, 2022, **926**, 116938.
68 Mayo Clinic Labtoratories, *SERU - Overview: Serotonin, 24 Hour, Urine*, **https://www.mayocliniclabs.com/test-catalog/Overview/87834**.
69 U. Andreasson, A. Perret-Liaudet, L. J. C. van Waalwijk van Doorn, K. Blennow, D. Chiasserini, S. Engelborghs, T. Fladby, S. Genc, N. Kruse, H. B. Kuiperij, L. Kulic, P. Lewczuk, B. Mollenhauer, B. Mroczko, L. Parnetti, E. Vanmechelen, M. M. Verbeek, B. Winblad, H. Zetterberg, M. Koel-Simmelink and C. E. Teunissen, *Front. Neurol.*, 2015, **6**, 179.